Nuclear Engineering and Technology 50 (2018) 97–106

Contents lists available at ScienceDirect

Nuclear Engineering and Technology

journal homepage: www.elsevier.com/locate/net

Original Article

Robust feedback-linearization control for axial power distribution in pressurized water reactors during load-following operation

M. Zaidabadi nejad, G.R. Ansarifar*

Department of Nuclear Engineering, Faculty of Advanced Sciences and Technologies, University of Isfahan, 81746-73441, Isfahan, Iran

ARTICLE INFO

Article history:
Received 10 May 2017
Received in revised form
24 October 2017
Accepted 24 October 2017
Available online 2 December 2017

Keywords:
Axial Offset
Dynamic Sliding Mode Control
Feedback-Linearization
Validated Four Nodes Kinetics Reactor Model

ABSTRACT

Improved load-following capability is one of the most important technical tasks of a pressurized water reactor. Controlling the nuclear reactor core during load-following operation leads to some difficulties. These difficulties mainly arise from nuclear reactor core limitations in local power peaking: the core is subjected to sharp and large variation of local power density during transients. Axial offset (AO) is the parameter usually used to represent the core power peaking. One of the important local power peaking components in nuclear reactors is axial power peaking, which continuously changes. The main challenge of nuclear reactor control during load-following operation is to maintain the AO within acceptable limits, at a certain reference target value.

This article proposes a new robust approach to AO control of pressurized water reactors during load-following operation. This method uses robust feedback-linearization control based on the multipoint kinetics reactor model (neutronic and thermal-hydraulic). In this model, the reactor core is divided into four nodes along the reactor axis. Simulation results show that this method improves the reactor load-following capability in the presence of parameter uncertainty and disturbances and can use optimum control rod groups to maneuver with variable overlapping.

1. Introduction

Controlling the nuclear reactor core during load-following operation is an important area in nuclear engineering, particularly in pressurized water reactors (PWRs) [5].

A nuclear reactor core has a multivariable nature and is a complex nonlinear system. Any power level change can induce unintended time–space xenon oscillations, resulting in large local power peaking. Such complexity cannot be duly represented by point kinetics models [12]. Therefore, a multipoint kinetics model, which is based on the nodal neutronic and thermal-hydraulic method, is a suitable choice for modeling the power axial oscillations. In the case of nodal methods, the reactor core is considered to be divided into a number of regions in which the neutron flux and material composition are treated as uniform. The regions are treated as smaller cores coupled through neutron flux [7]. Avery [4] and Komata [11] described the basic idea of the multipoint kinetic model. Kobayashi [10] has used unperturbed flux to calculate kinetics parameters for multipoint kinetics equations.

Furthermore, central to the method are the values of the coupling coefficients. In load-following mode, the reactor should track the demand load changes while considering the core limitations in safety margins and local power peaking.

Axial offset (AO) is the parameter usually used to represent the core power peaking, this is a practical parameter that is defined as the actual axial power distribution in the core, which varies significantly. In previous classical control systems, usually crisp logics have been used to control the thermal power and AO. However, in the constant AO strategy the reactor AO is maintained within predetermined limits via suitable maneuvering of the control rods. Thus, using robust control based on the multipoint kinetics model is more suited to this type of problem and may improve the load-following capability. Modern intelligent techniques, using sliding mode control, allow us to satisfactory handle such a problem [3], but only at the expense of high gains [21]. Indeed, the main obstacles for application of sliding mode control are two interconnected phenomena: chattering and high activity of control action. It is well known that the amplitude of chattering is proportional to the magnitude of any discontinuous control. Especially, to achieve perfect tracking and stability in the presence of parameter uncertainty, external disturbance, and measurement noise, the magnitude of the sliding mode control should be increased,

* *Corresponding author.*
E-mail address: ghr.ansarifar@ast.ui.ac.ir (G.R. Ansarifar).

https://doi.org/10.1016/j.net.2017.10.013

which leads to high chattering phenomena. Besides this, boundary layer thickness expansion to decrease the chattering phenomena leads to large steady output tracking error. These two problems can be handled simultaneously if the magnitude of the control is reduced. In this article, a new robust approach based on feedback-linearization control is used to obtain the minimum possible value of control and to decrease both the chattering phenomena and the boundary layer thickness expansion, which exhibits large steady output tracking error, leading to external disturbances and parameters uncertainty.

This article, for the first time, presents a robust feedback-linearization controller using the Lyapunov approach based on the multipoint kinetics reactor model. Indeed, the purpose of this article is to present a robust feedback-linearization control system for the load-following operations of nuclear reactors such that oscillations of axial power distribution are bounded within acceptable limits, which will improve the performance of the conventional feedback-linearization and nonlinear sliding mode control techniques. The motivation of modeling the robust feedback-linearization controller for power offset is its simplicity, ease of implementation in practical applications, and improvement of the performance and robustness of conventional feedback-linearization in the face of external disturbances and parameter uncertainty; another motivation is improvement of the nonlinear sliding mode control techniques while obtaining a minimum possible value of control and decreasing both chattering phenomena and boundary layer thickness expansion in the face of external disturbances and parameter uncertainty. One of the important advantages of the presented robust feedback linearization technique is its simplicity. Indeed, contributions of the proposed approach in this article are (1) improvement of the performance and robustness of the conventional feedback-linearization technique in the face of external disturbances and parameter uncertainty by combining dynamic sliding mode control and conventional feedback-linearization, (2) improvement of the nonlinear sliding mode control technique while obtaining the minimum possible value of control and decreasing both chattering phenomena and boundary layer thickness expansion in the face of external disturbances and parameter uncertainty. Indeed, in this article, chattering phenomena, which are the main obstacles for application of sliding mode control in the face of external disturbances and parameter uncertainty, are removed by combining dynamic sliding mode control and conventional feedback-linearization.

The simulation results demonstrate the effectiveness of the proposed control system in diverse operating conditions. Also, the article shows that this controller may improve the responses, compared to conventional proportional integral derivative (PID) controller, conventional feedback-linearization and nonlinear sliding mode control techniques.

2. Nuclear reactor model

As discussed above, the point kinetics model is not valid in the case of PWRs because the neutron flux shape undergoes appreciable variation with time, and this model cannot analyze the power axial oscillations [9]. Besides this, control of the axial power distribution is essential during load-following operation in nuclear reactors. Therefore, the multipoint kinetics model, which is based on the nodal method, is a good choice for modeling power axial oscillations [4]. To use the multipoint method, the reactor core is considered to be divided into a number of nodes along the reactor axis, in which the material composition and neutron flux are treated as uniform. Furthermore, the nodes are treated as small cores coupled through neutron diffusion; central to the method are the values of the coupling coefficients.

To simulate the nuclear reactor core, a multipoint kinetics model with four nodes is selected as the validated multipoint kinetics model [21]. Therefore, the PWR core is considered to be divided into four nodes along the reactor axis, as shown in Fig. 1.

To simulate the nuclear reactor core, with respect to an equilibrium condition, the normalized model, based on the four points kinetics equations with three delayed neutron groups, based on the Skinner–Cohen model, which has been validated and benchmarked [9], is used. The utilized normalized neutron kinetics model is as follows [21]:

$$\frac{dn_{ri}}{dt} = \frac{\rho_i - \beta}{l_i} n_{ri} + \sum_{k=1}^{3} \frac{\beta_k}{l_i} C_{ri,k} - \alpha_{ii} \frac{n_{ri}}{l_i} + \sum_{\substack{j=1 \\ j \neq i}}^{N} \frac{\alpha_{ji}}{l_i} n_{rj}, i = 1, \ldots, 4 \quad (1)$$

$$\frac{dC_{ri,1}}{dt} = \lambda_1 n_{ri} - \lambda_1 C_{ri,1}, \quad (2)$$

$$\frac{dC_{ri,2}}{dt} = \lambda_2 n_{ri} - \lambda_2 C_{ri,2}, \quad (3)$$

$$\frac{dC_{ri,3}}{dt} = \lambda_3 n_{ri} - \lambda_3 C_{ri,3}, \quad (4)$$

$$\frac{d\rho_{r1}}{dt} = \frac{G_r Z_{r1}}{2} \left(1 - sign\left(h_1 - \frac{h_0}{4}\right)\right) \quad (5)$$

$$\frac{d\rho_{r2}}{dt} = \frac{G_r Z_{r1}}{2} \left(1 + sign\left(h_1 - \frac{h_0}{4}\right)\right) \quad (6)$$

$$\frac{d\rho_{r3}}{dt} = \frac{G_r Z_{r2}}{2} \left(1 - sign\left(h_2 - \frac{3h_0}{4}\right)\right) \quad (7)$$

$$\frac{d\rho_{r4}}{dt} = \frac{G_r Z_{r2}}{2} \left(1 + sign\left(h_2 - \frac{3h_0}{4}\right)\right) \quad (8)$$

$$\frac{dh_1}{dt} = h_0 Z_{r1} \quad (9)$$

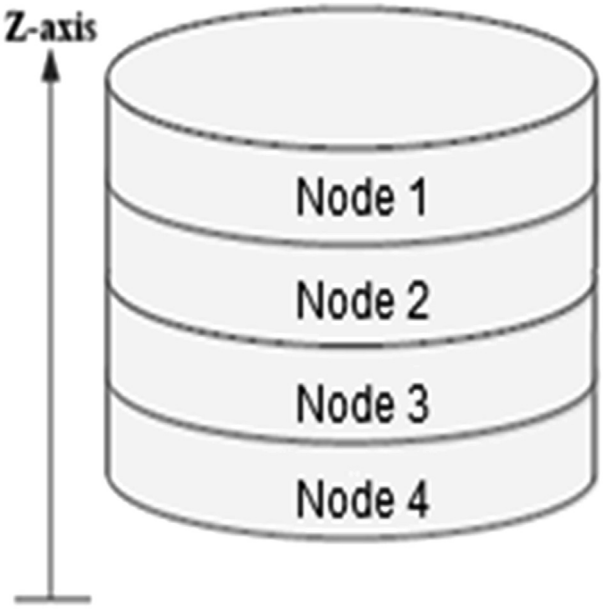

Fig. 1. Nodalization of the PWR reactor core in the axial direction.
PWR, pressurized water reactor.

$$\frac{dh_2}{dt} = h_0 Z_{r2} \tag{10}$$

where n_{ri}, $C_{ri,k}$, G_r, Z_{r1}, Z_{r2}, α_{ii}, α_{ji}, and h_0 are the neutron density relative to the initial equilibrium density in node i (relative power level in node i), the k^{th} group relative precursor density normalized with the initial equilibrium density in node i, the total reactivity value of the control rod, the control rod speed (fraction of core length per second) at the top and bottom of the core, the coupling coefficient of the i^{th} axial node to itself, the coupling coefficients between the i^{th} axial node and the other nodes, and the total core height, respectively. The reactor power in node i can be calculated as follows:

$$P_i(t) = P_0 n_{ri}(t) \tag{11}$$

where P_0 is the nominal power (MW) and n_r follow as:

$$n_r = \frac{n_{r1} + n_{r2} + n_{r3} + n_{r4}}{4} \tag{12}$$

Eqs. (5)–(8) demonstrate that reactivity insertion at the top of the core is affected by the first control rod banks, which are assumed to travel through the top, and reactivity insertion at the bottom of the core is affected by the second control rod bank, which is assumed to travel through the bottom of the core.

Xenon-135 (^{135}Xe) is the most important of the thermal fission products; it has large absorption cross-section for thermal neutrons. The concentration of xenon depends on the iodine concentration. The equations related to the changes of iodine and xenon concentration for each node in the four point kinetic model are as follows:

$$\frac{dI_i}{dt} = \frac{\gamma_I P_i}{GV_i} - \lambda_I I_i, i = 1, 2, \ldots, 4 \tag{13}$$

$$\frac{dX_i}{dt} = \frac{\gamma_X P_i}{GV_i} + \lambda_I I_i - \left(\lambda_X + \frac{\sigma_a^X P_i}{G\Sigma_f V_i}\right) X_i, i = 1, 2, \ldots, 4 \tag{14}$$

In a simple case, the lumped influences of coolant and fuel temperature are taken into account for each node [1]. The respective energy balance equations for coolant and fuel in each axial node can be defined as follows [20,21]:

$$\frac{dT_{fi}}{dt} = \frac{1}{\mu_{fi}}\left[fP_i - \Omega_i\left(T_{fi} - T_{ci}\right)\right], i = 1, 2, \ldots, 4 \tag{15}$$

$$\frac{dT_{ci}}{dt} = \frac{1}{\mu_{ci}}\left[(1-f)P_i + \Omega_i\left(T_{ft} - T_{ci}\right) - 2M_i(T_{ci} - T_{ci,in})\right], \quad i = 1, 2, \ldots, 4 \tag{16}$$

where T_{fi}, $T_{ci,\,in}$, and T_{ci} are fuel temperature in node i, the coolant inlet temperature in node i, and the average coolant temperature in node i, respectively. Also, μ_{ci}, Ω_i, and M_i are not constants. The following equations show the dependence of these variables on the relative power level at t = 0 [13]:

$$\mu_{ci} = \left(\frac{160}{9} n_{r0,i} + 54.022\right) MW \cdot \frac{s}{^\circ C} \tag{17}$$

$$\Omega_i = \left(\frac{5}{3} n_{r0,i} + 4.93333\right) MW \cdot \frac{s}{^\circ C} \tag{18}$$

$$M_i = (28 n_{r0,i} + 74) \frac{MW}{^\circ C} \tag{19}$$

where $n_{r0,i}$ is total relative power level at t = 0 in node i.

Thermal reactivity feedbacks for each node are defined as follows [9,13]:

$$\rho_{fTi} = \alpha_{fi}\left(T_{fi} - T_{f0,i}\right) + \alpha_{ci}\left(T_{ci} - T_{c0,i}\right) \tag{20}$$

where

$$\alpha_{fi} = (n_{r0,i} - 4.24) \times 10^{-5} \left.\frac{\delta k}{k}\right/ ^\circ C \tag{21}$$

$$\alpha_{ci} = (-4 n_{r0,i} - 17.3) \times 10^{-5} \left.\frac{\delta k}{k}\right/ ^\circ C \tag{22}$$

α_{ci} and α_{fi} are the thermal reactivity coefficients of the coolant and the fuel, respectively, at node i.

In this article, the model assumes feedback from lumped fuel and coolant temperatures in each node. Poisson reactivity feedback for each node of the core is defined as [13]:

$$\rho_{fpi} = -\frac{\sigma_a^X (X_i - X_{0i})}{\nu\Sigma_f}, i = 1, 2, \ldots, 4 \tag{23}$$

Also, total reactivity for each node of the core (ρ_i), which is used in Eq. (1), is as follows:

$$\rho_i = \rho_{ri} + \rho_{fpi} + \rho_{fTi}, i = 1, 2, \ldots, 4 \tag{24}$$

Local power peaking in nuclear reactors is a complex phenomenon, resulting from different reactor parameters such as xenon oscillation. While axial power peaking continuously changes, radial power peaking usually flattens once at the beginning of cycle. AO is the parameter usually used to determine the core peaking power. This parameter is used as the performance index to evaluate the spatial distortions of power and is defined as the difference between the powers generated in the upper and the lower halves of the core as follows [8]:

$$AO = \frac{P_t - P_b}{P_t + P_b} \tag{25}$$

where P_t and P_b are the integrated powers in the top and bottom halves of the core, respectively. Since AO is defined as the normalized difference between the powers in the top and bottom halves of the core, the reactor core is considered to be axially divided into an even number of nodes, namely 4 nodes.

During load-following operation, the AO should be kept within a control band (target boundaries) near a reference AO value that corresponds to the most stable axial power distribution possible for existing core condition, that is, the power shape that exists at full power with equilibrium xenon and no control rods in the core [8].

Axial xenon oscillation (AX) is defined as the difference between the xenon concentrations in the top and bottom halves of the core in the axial direction, as follows [8]:

$$AX = \frac{X_t - X_b}{X_{t0} + X_{b0}} \tag{26}$$

where X_t and X_b are the xenon concentration in the upper and lower halves of core, respectively, and X_0 is the equilibrium xenon

concentration at full reactor power. This index shows the normalized difference between the xenon concentration in the upper and lower halves of the reactor core. The main challenge of the reactor control, during load-following operation, is to maintain AX and AO within certain limits, near a reference target value.

The limitation on the AO can be analyzed in $P_r - \Delta I$ coordinates, where ΔI is the normalized AO and is defined as:

$$\Delta I = AO \times P_r \tag{27}$$

ΔI represents the difference between the power at the bottom and top of the core as a fraction of the full power. The limitations on AO can be shown by the two parallel lines in $P_r - \Delta I$ coordinates [16]. This means that the core working conditions in $P_r - \Delta I$ coordinates must lie within a certain band (e.g. 5%) during any power transient.

To evaluate the performance of the designed controller structure, a set of simulations is performed on the VVER-1000 nuclear reactor. VVER-1000 (Russian type of PWRs) was developed on the basis of the proven performance of PWRs with annular fuel plates that have hexagonal configuration and 1/6 symmetric shape. The core consists of 163 fuel assemblies (FAs); each FA is comprised of 311 fuel rods and 18 guiding channels for control rods or burnable poisons. The VVER-1000 generates 3000 MW at full power and there are six control rods with regulating function, the so-called group H10. Important physical and dynamic parameters of the VVER-1000 are given in Table 1 [14].

3. Derivation controller design for PWR nuclear reactors

In this section, a brief description of the relevant theory and control design algorithms used in the development of the PWR controller is given.

3.1. Conventional feedback-linearization control

Feedback linearization is a common approach used in controlling nonlinear systems. Feedback linearization may be applied to nonlinear systems of the form:

$$\begin{cases} \dot{x}(t) = f(x) + g(x)u \\ \mathrm{y} = \mathrm{h(x)} \end{cases} \tag{28}$$

where x is a state vector, u is a control function and y is a controlled output.

The feedback linearization technique is based on the linearized relationship between input and output. It is composed of two controller loops, an inner loop (nonlinear controller) for eliminating nonlinear terms of model dynamics and an outer loop (linear controller) for control of the linearized model.

Also, the system described by Eq. (28) has relative degree r if [3]:

$$\begin{cases} L_g L_f^k h(x) = 0, \quad k < r-1 \\ L_g L_f^{r-1} h(x) \neq 0 \end{cases} \tag{29}$$

where $L_p h(x) = \frac{\partial h(x)}{\partial x}.p$ for $p = f, g$ is the Lie derivative of the function $h(x)$ [18].

Considering this definition of relative degree in light of the expression of the time derivative of the output y, we can consider the relative degree of system (28) as the number of times we have to differentiate the output y before the input u appears explicitly.

In this article, according to the four-point kinetics equations that were described in Section 2 and considering the two control rods speeds Z_{r1} and Z_{r2}, as the control inputs and considering the relative power in each node as the control outputs, the relative degree of the reactor system is 2 and, therefore, at the first step of controller design, the desirable two-control law according to feedback-linearization can be represented as follows:

$$\ddot{y}_1 = \ddot{n}_{rt} = \ddot{n}_{rdt} - \eta_t e_t - \eta_1 \dot{e}_t \tag{30}$$

$$\ddot{y}_2 = \ddot{n}_{rb} = \ddot{n}_{rdb} - \eta_t e_b - \eta_2 \dot{e}_b \tag{31}$$

where $\eta_t, \eta_b, \eta_1, \eta_2$ are strictly positive constants and:

$$e_t = n_{rt} - n_{rdt} = \frac{n_{r1} + n_{r2}}{2} - \frac{n_{r1d} + n_{r2d}}{2} \tag{32}$$

$$e_b = n_{rb} - n_{rdb} = \frac{n_{r3} + n_{r4}}{2} - \frac{n_{r3d} + n_{r4d}}{2} \tag{33}$$

Using Eqs. (1),(30),(31), control inputs are obtained as follows:

$$Z_{r1} = \frac{2l}{(n_{r1}+n_{r2})G_r}\left[\frac{\ddot{n}_{r1d}+\ddot{n}_{r2d}}{2} - \eta_t e_t - \eta_1 \dot{e}_t - \frac{\left(\rho_1 + \frac{\rho_{r1}}{2} + \rho_2 + \frac{\rho_{r2}}{2}\right) - \beta}{4l}(\dot{n}_{r1}+\dot{n}_{r2}) - \sum_{k=1}^{3}\frac{\beta_i}{2l}\left(\dot{C}_{r1,k}+\dot{C}_{r2,k}\right) + \frac{1}{2l}\left(\frac{\alpha_{11}\dot{n}_{r1}+\alpha_{22}\dot{n}_{r2}}{2} - \frac{\alpha_{33}\dot{n}_{r3}+\alpha_{44}\dot{n}_{r4}}{2}\right)\right] - \frac{1}{2G_r}\left[\alpha_{f1}\frac{dT_{f1}}{dt} + \alpha_{f2}\frac{dT_{f2}}{dt} + \alpha_{c1}\frac{dT_{c1}}{dt} + \alpha_{c2}\frac{dT_{c2}}{dt} - \frac{\sigma_a^X}{\nu\Sigma_f}(\dot{x}_1+\dot{x}_2)\right] \tag{34}$$

$$Z_{r2} = \frac{2l}{(n_{r3}+n_{r4})G_r}\left[\frac{\ddot{n}_{r3d}+\ddot{n}_{r4d}}{2} - \eta_b e_b - \eta_2 \dot{e}_b - \frac{\left(\rho_3 + \frac{\rho_{r3}}{2} + \rho_4 + \frac{\rho_{r2}}{2}\right) - \beta}{4l}(\dot{n}_{r3}+\dot{n}_{r4}) - \sum_{k=1}^{3}\frac{\beta_i}{2l}\left(\dot{C}_{r3,k}+\dot{C}_{r4,k}\right) + \frac{1}{2l}\left(\frac{\alpha_{33}\dot{n}_{r3}+\alpha_{44}\dot{n}_{r4}}{2} - \frac{\alpha_{11}\dot{n}_{r1}+\alpha_{22}\dot{n}_{r2}}{2}\right)\right] - \frac{1}{2G_r}\left[\alpha_{f3}\frac{dT_{f3}}{dt} + \alpha_{f4}\frac{dT_{f4}}{dt} + \alpha_{c3}\frac{dT_{c3}}{dt} + \alpha_{c4}\frac{dT_{c4}}{dt} - \frac{\sigma_a^X}{\nu\Sigma_f}(\dot{x}_3+\dot{x}_4)\right] \tag{35}$$

3.2. Robust feedback-linearization control

Many real-life control systems are nonminimum phase in nature. A nonlinear control system is nonminimum phase if the corresponding internal or zero dynamics are unstable (Isidori, 1989). Particularly, a linear single input–single output (SISO) system is nonminimum phase if an input–output transfer function has zeroes in the right half of the complex plane. The application of powerful nonlinear control techniques such as feedback

Table 1
Parameters of the nuclear reactor at 100% nominal power.

Parameter	Value	Parameter	Value
Thermal power	3000 MW	β_1	0.0002145
Core height in the working state (cm)	355 cm	β_2	0.002249
Core equivalent diameter (cm)	316 cm	β_3	0.0040365
Coolant inlet temperature (°C)	291°C	Decay constant of X (λ_x)	2.08×10^{-5} s^{-1}
Coolant flow rate (kg/s)	16,704 kg/s	Decay constant of I (λ_I)	2.88×10^{-5} s^{-1}
Diffusion constant (D)	0.16 cm	Fractional fission yield of X (γ_x)	0.00228
Mean velocity of thermal neutron (ν)	2.2×10^5 cm/s	Fractional fission yield of I (γ_I)	0.0639
Effective prompt neutron life time (l)	2×10^{-5} s	Total reactivity worth of control rod (G_r)	14.5×10^{-3}
Microscopic absorption cross-section of X	2.36×10^{-18} cm^2	Microscopic fission cross section	0.3358 cm^{-1}

linearization is restricted by the nonminimum phase nature of a plant [19,6]. Accordingly, for any bounded control, the existence condition of conventional feedback linearization cannot be entirely met and instability can be experienced by the system because of the unstable internal dynamics. To solve this problem, the problem of output tracking in nonlinear nonminimum phase systems has been proposed in a study by Shtessel [15] using a dynamic sliding mode controller, as follows:

$$\begin{cases} \dot{x} = Ax + bu \\ y = Gx \end{cases} \tag{36}$$

where A, b and G are constant matrices of corresponding dimensions and {A, b} is a controllable pair. The first step of dynamic sliding mode controller design, the dynamic sliding manifold, can be introduced as follows:

$$\tau = u + \sigma = 0 \tag{37}$$

The function σ is a dynamic operator.

Remark 1. Existence condition of sliding mode $\tau\dot{\tau} < -\eta|\tau|$ must be satisfied in the vicinity of the sliding manifold [6].

Assuming that the dynamic sliding mode exists, the equation of sliding motion of the system in the dynamic sliding manifold (Eq. (37)) can be governed by:

$$\begin{cases} \dot{x} = A_{11}x - A_{12}\sigma \\ y = G_1x - G_2\sigma \end{cases} \tag{38}$$

The plant described by Eq. (38) with control input σ and output y is a nonminimum phase system.

The function σ is a dynamic compensator for stabilizing internal dynamics [2]. The sliding manifold is reached in a finite time $t_r = \frac{|\tau(0)|}{\eta}$ and the system's trajectory stays on the manifold thereafter when $\tau(0)$ is an initial value of a sliding manifold and $\eta > 0$. To satisfy the existence condition of the sliding mode on the dynamic sliding manifold (Eq. (37)), the control function u is given in the following way:

$$\dot{u} = -u + u_c \tag{39}$$

$$u_c = -[\eta sign(\tau) + \dot{\sigma} - u] \tag{40}$$

The discontinuous control law is designed in a simplified manner:

$$u_c = -U_{max} sign(\tau) \tag{41}$$

where

$$\begin{cases} U_{max} > (|u_{eq}| + \eta) \\ u_{eq} = \dot{\sigma} - u \end{cases} \tag{42}$$

To avoid control chattering, discontinuous control (Eq. (41)) is realized in a smooth form as [17]:

$$u_c = -U_{max} tanh\left(\frac{\tau}{\varphi}\right) \tag{43}$$

where φ is the width of the boundary layer that is introduced about the origin in the τ-space.

At the second step of controller design, the desirable two control law according to feedback-linearization is combined with dynamic sliding mode and a robust control law, represented as follows:

$$\tau_t = u_t + \sigma_t = 0 \Rightarrow \sigma_t = -u_t \tag{44}$$

$$\tau_b = u_b + \sigma_b = 0 \Rightarrow \sigma_b = -u_b \tag{45}$$

where:

$$u_t = (\rho_{r1} + \rho_{r2}) \tag{46}$$

$$u_b = (\rho_{r3} + \rho_{r4}) \tag{47}$$

Also, σ_t and σ_b are designed as follows:

$$\begin{aligned} \dot{n}_{rt} = \dot{n}_{rdt} - \eta_t e_t \Rightarrow \frac{\dot{n}_{r1} + \dot{n}_{r2}}{2} = \frac{\dot{n}_{r1d} + \dot{n}_{r2d}}{2} - \eta_t e_t \Rightarrow \sigma_t \\ = -\frac{2l}{(n_{r1} + n_{r2})}\left[\frac{\ddot{n}_{r1d} + \ddot{n}_{r2d}}{2} - \eta_t e_t - \sum_{k=1}^{3}\frac{\beta_i}{2l}(C_{r1,k} + C_{r2,k}) + \frac{1}{2l}\left(\frac{\alpha_{11}n_{r1} + \alpha_{22}n_{r2}}{2} - \frac{\alpha_{33}n_{r3} + \alpha_{44}n_{r4}}{2}\right)\right] \\ + \frac{1}{2}\left[\alpha_{f1}\left(T_{f1} - T_{f01}\right) + \alpha_{f2}\left(T_{f2} - T_{f02}\right) + \alpha_{c1}(T_{c1} - T_{c01}) + \alpha_{c2}(T_{c2} - T_{c02}) - \frac{\sigma_a^X}{\nu\Sigma_f}\left(\frac{(X_1 - X_{01}) + (X_2 - X_{02})}{2}\right)\right] + \beta \end{aligned} \tag{48}$$

$$\dot{n}_{rb} = \dot{n}_{rdb} - \eta_b e_b \Rightarrow \frac{\dot{n}_{r3} + \dot{n}_{r4}}{2} = \frac{\dot{n}_{r3d} + \dot{n}_{r4d}}{2} - \eta_b e_b \Rightarrow \sigma_b$$
$$= -\frac{2l}{(n_{r3} + n_{r4})}\left[\frac{\ddot{n}_{r3d} + \ddot{n}_{r4d}}{2} - \eta_b e_b - \sum_{k=1}^{3}\frac{\beta_i}{2l}(C_{r3,k} + C_{r4,k}) + \frac{1}{2l}\left(\frac{\alpha_{33}n_{r3} + \alpha_{44}n_{r4}}{2} - \frac{\alpha_{11}n_{r1} + \alpha_{22}n_{r2}}{2}\right)\right]$$
$$+\frac{1}{2}\left[\alpha_{f3}\left(T_{f3} - T_{f03}\right) + \alpha_{f4}\left(T_{f4} - T_{f04}\right) + \alpha_{c3}(T_{c3} - T_{c03}) + \alpha_{c4}(T_{c4} - T_{c04}) - \frac{\sigma_a^X}{\nu\Sigma_f}\left(\frac{(X_3 - X_{03}) + (X_4 - X_{04})}{2}\right)\right] - \beta \quad (49)$$

According to Eq. (39), the control rod reactivity in the reactor core (u) is related to the control rod speeds (u_c) and, according to Eq. (43), to satisfy the existence condition of the sliding mode on the dynamic sliding manifolds, control rod speeds as control inputs are given as follows:

$$Z_{r1} = -100^{*}tanh\left(\frac{\tau_t}{\varphi}\right) \quad (50)$$

$$Z_{r2} = -100^{*}tanh\left(\frac{\tau_b}{\varphi}\right) \quad (51)$$

4. Simulation results

In this section, to evaluate the robustness and performance of the designed controller structure, a set of simulations is performed on the nuclear reactor model described in Sections 2 and 3.

Simulation for 50%→40%→50% demand power level change; all parameters are perturbed by +30% from their nominal values with external disturbance of the control rod speed. The results show that the robustness and stability have indeed been achieved. Also, the desired power is reached quickly with no oscillation or overshoot.

4.1. Reactor relative power

Desired relative power level and actual core thermal relative power are shown in Fig. 2.

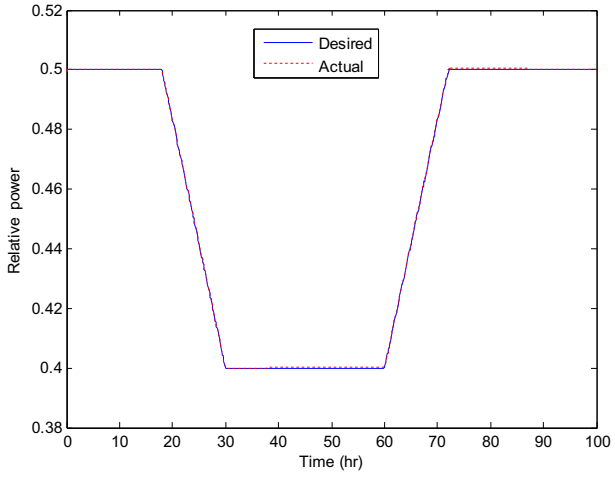

Fig. 2. Desired relative power level and actual core thermal relative power with uncertainty and external disturbance.

4.2. Total reactivity

Total reactivity in the each node of the reactor core is shown in Fig. 3, which has been calculated based on Eq. (24) and is the summation of the control rod reactivity (ρ_{ri}), thermal reactivity feedback (ρ_{fTi}), and poison reactivity feedback (ρ_{fpi}) for each node of the core.

4.3. Control rod speed

Control rod speeds in the top and bottom of the reactor core as control inputs are shown in Fig. 4; values have been calculated based on Eqs.(50) and (51).

4.4. Normalized axial offset

The core ΔI is limited to −10% P_r (1 ± 5%), where −10% corresponds to the AO at the nominal power. Fig. 5 shows real core ΔI and core ΔI limitations in P_r−ΔI coordinate. In this figure, red line is real core normalized axial offset and dashed black lines is the its bounded lines.

These figures show that ΔI is bounded within acceptable limits during load-following operation.

4.5. Xenon concentrations for each node

Xenon concentrations in each node of the reactor core are shown in Fig. 6. Owing to Eq. (14), decreasing the reactor power leads to a decrease of the burning of xenon. Therefore, xenon concentrations increase. Also, when the power increases, the burning of materials also increases and then xenon concentration decreases. So, xenon concentration behavior is inversely proportional to the power behavior presented in Fig. 2. The results show that xenon concentration is bounded during load-following operation.

4.6. Axial xenon oscillation and axial offset

AX and AO of the reactor core are shown in Fig. 7.

Simulation results show that perfect tracking, stability, and bounded AO during load-following operation have been achieved in the presence of parameter uncertainty and external disturbance. Also, AX in the reactor is bounded.

4.7. Average fuel and coolant temperature

Average fuel and coolant temperature are shown in Fig. 8 as follows:

Changes in the fuel temperature and coolant temperature are proportional to the change in reactor power based on the Eqs.(15) and (16). Therefore, changes in the fuel temperature and coolant temperature are proportional to changes in the reactor power behavior, as shown in Fig. 2.

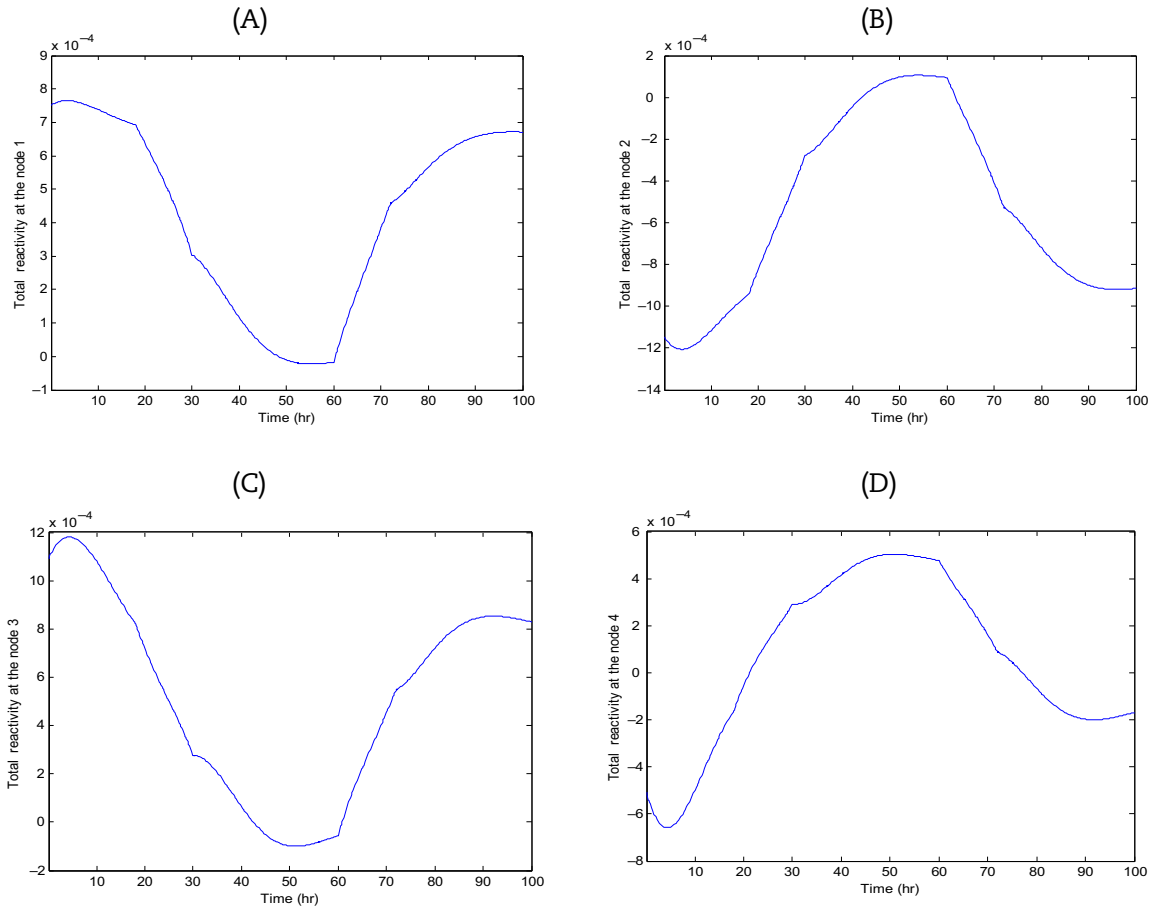

Fig. 3. Total reactivity. (A) At node 1. (B) At node 2. (C) At node 3. (D) At node 4.

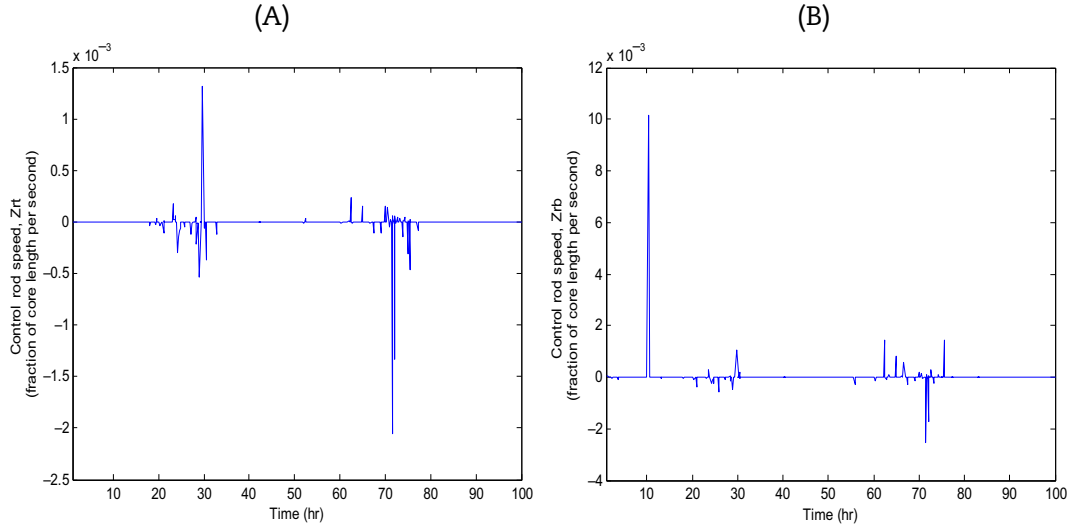

Fig. 4. Control rod speed. (A) At the top of the reactor. (B) At the bottom of the reactor.

5. Comparison of the presented robust controller with PID controller, conventional feedback-linearization, and sliding mode control in the presence of the parameter uncertainty and external disturbance

In this section, to clearly show the superiority and performance of the presented robust controller, a comparison between the designed robust feedback-linearization, PID controller, conventional feedback-linearization, and nonlinear sliding mode control technique has been done in the presence of parameter uncertainty and external disturbance. The robust feedback-linearization, PID controller, and conventional feedback-linearization results for reactor relative power with uncertainty and external disturbance are presented in Fig. 9.

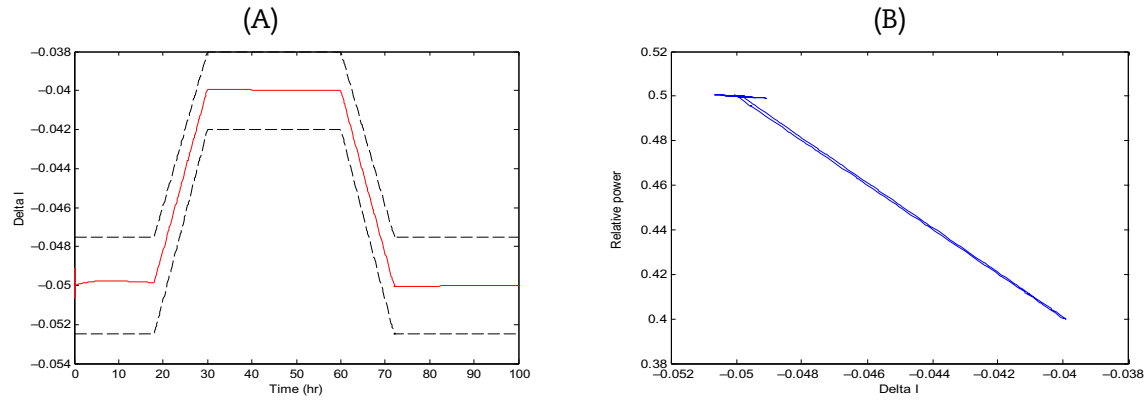

Fig. 5. (A) Normalized axial offset (ΔI). (B) Core ΔI in P_r–ΔI coordinates.

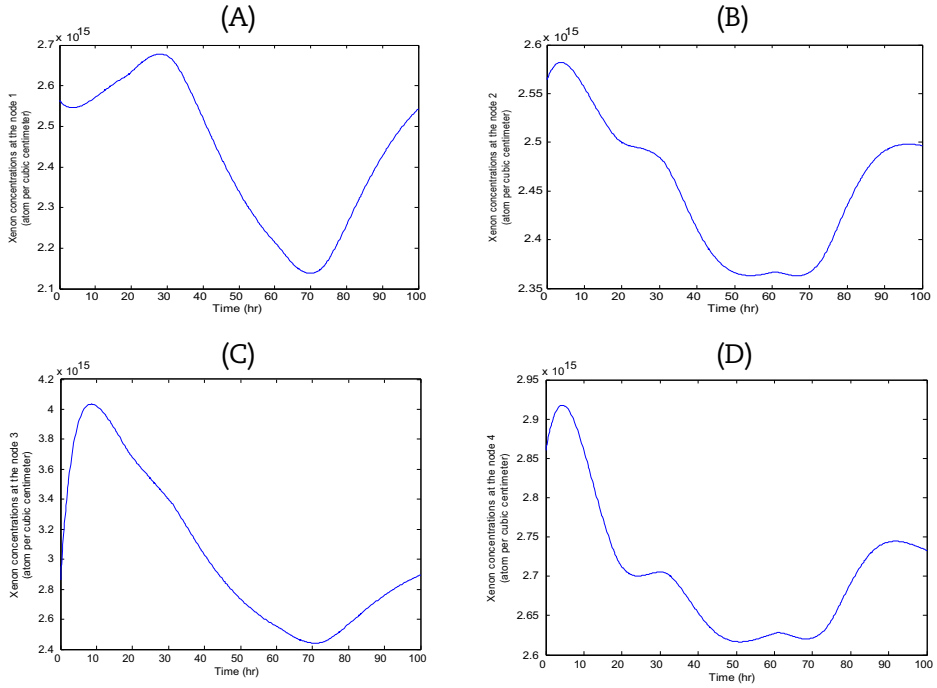

Fig. 6. Xenon concentrations. (A) At node 1. (B) At node 2. (C) At node 3. (D) At node 4.

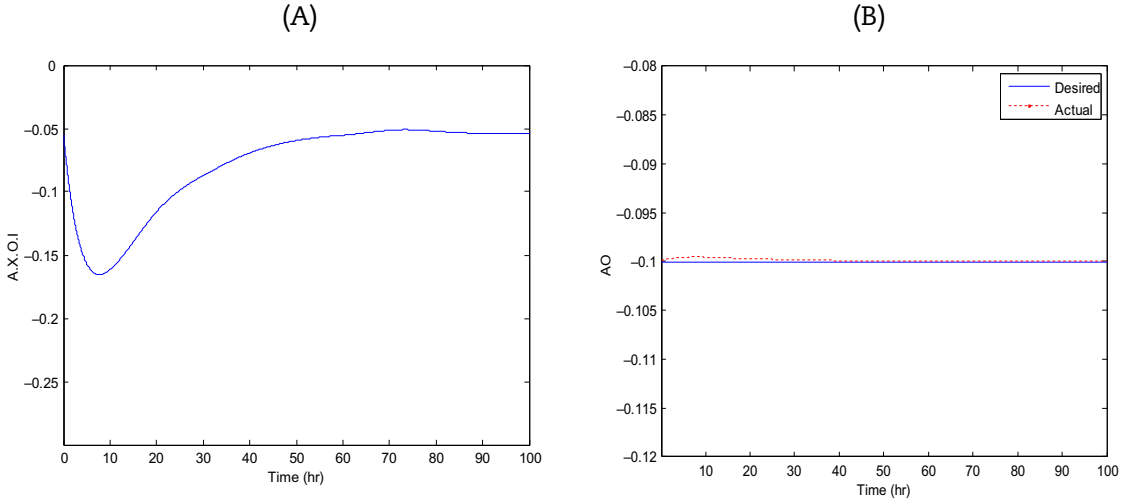

Fig. 7. (A) Axial xenon oscillation in the reactor, AX. (B) Axial offset in the reactor, AO.

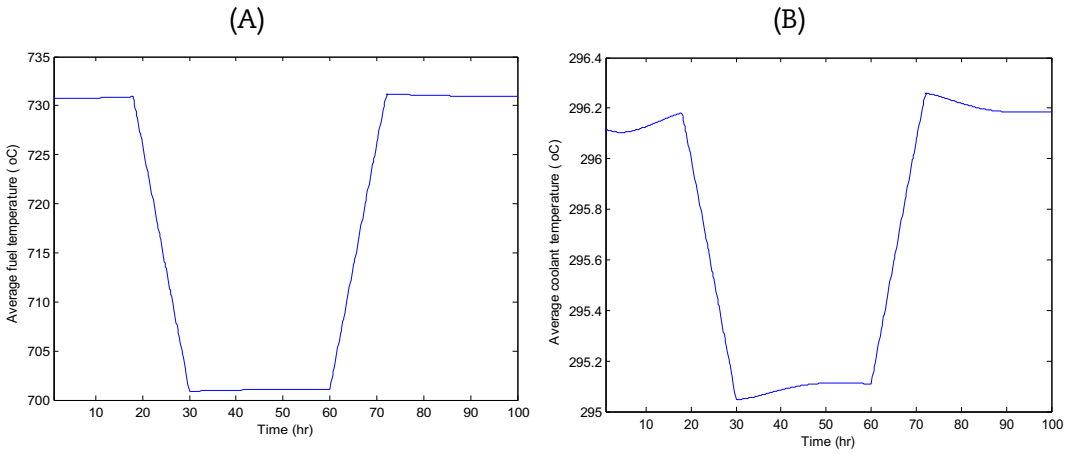

Fig. 8. (A) Average fuel temperature. (B) Average coolant temperature.

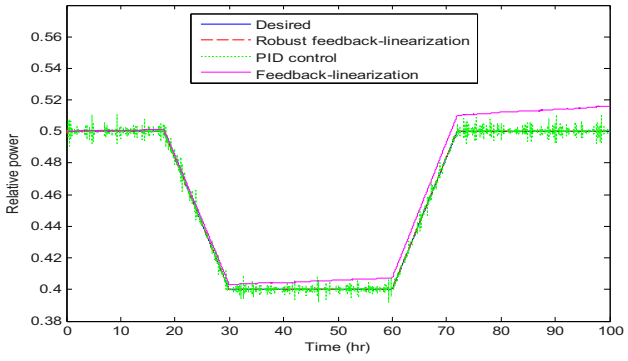

Fig. 9. Comparison between proposed robust feedback-linearization, PID control, and conventional feedback-linearization of reactor relative power.

Robust feedback-linearization and sliding mode control results of reactor relative power and normalized AO (ΔI) with uncertainty and external disturbance are presented in Figs. 10 and 11.

Results show a significant improvement in the load-following and an increased robustness for the proposed robust feedback-linearization compared to the PID controller, conventional feedback-linearization, and sliding mode control in the presence of the parameter uncertainty and external disturbance. Also, chattering phenomena have been removed by combining dynamic sliding mode control and conventional feedback-linearization.

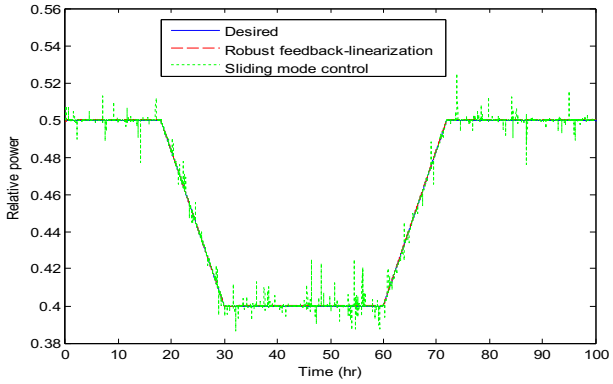

Fig. 10. Comparison between proposed robust feedback-linearization and sliding mode control of reactor relative power.

6. Conclusions

This article developed a new method to tackle the load-following operation with bounded AO as one of the important problems of modern PWRs. Improvement of load-following capability of plants using robust feedback-linearization control based on a multipoint kinetics reactor model (neutronic and thermal-hydraulic) has been achieved.

The reactor core was simulated based on four-point kinetics equations and three delayed neutron groups. In this model, instead of using a continuous space-dependent diffusion equation, discreet point kinetics equations were used. The method is based on dividing the reactor core into two nodes that are coupled through neutron diffusion; central to the method are the values of the coupling coefficients.

The results show that robust feedback-linearization succeeded at controlling the core AO within the specified bands during severe load-following operation. As a main contribution of the approach proposed in this article, performance and robustness of the conventional feedback-linearization technique in the face of external disturbances and parameter uncertainty have been improved by combining dynamic sliding mode control and conventional feedback-linearization. Also in this article, by combining dynamic sliding mode control and conventional feedback-linearization chattering phenomena, the main obstacles for application of sliding mode control in the face of external disturbances and parameter uncertainty have been removed by obtaining the minimum possible value of control and boundary layer thickness decrease in the face of external disturbances and parameter uncertainty.

The research presented in this article has investigated the feasibility of applying robust feedback-linearization control to nuclear reactors. The results presented in this article show that the load-following operation and axial power distribution can be well-controlled using the robust control with feedback-linearization methodology in nuclear reactors in the presence of model uncertainties and disturbance. Also, results show a significant improvement in the load-following and an increased robustness for the proposed robust feedback-linearization compared to the PID controller, conventional feedback-linearization, and sliding mode control.

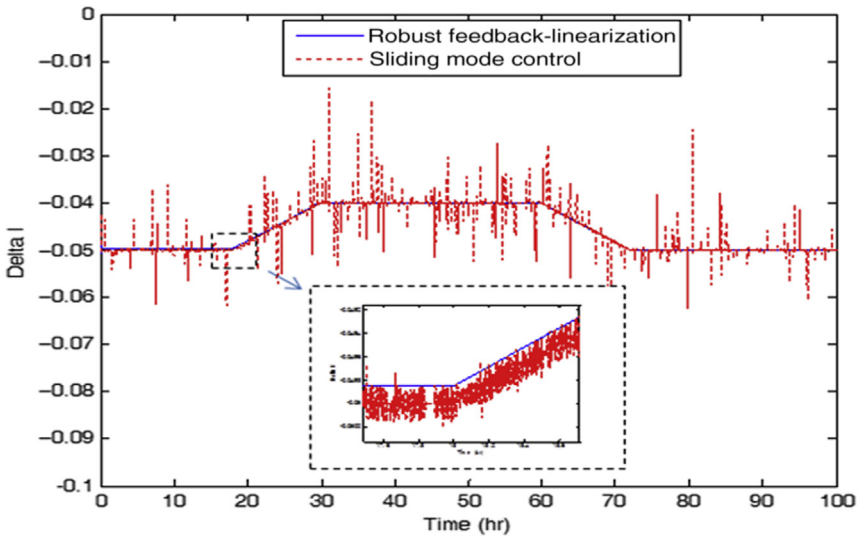

Fig. 11. Comparison between proposed robust feedback-linearization and sliding mode control of normalized axial offset (ΔI).

Conflicts of interest

All authors have no conflicts of interest to declare.

References

[1] H. Anglart, Nuclear Reactor Dynamics and Stability Lecture. Nuclear Reactor Technology, Department of Physics, School of Engineering Sciences, KTH, Stockholm, Sweden, 2011.
[2] G.R. Ansarifar, Control of the nuclear steam generators using adaptive dynamic sliding mode method based on the nonlinear model, Ann. Nucl. Energy 88 (2016) 280–300.
[3] G.R. Ansarifar, H.R. Akhavan, Sliding mode control design for a PWR nuclear reactor using sliding mode observer during load-following operation, Ann. Nucl. Energy 75 (2015) 611–619.
[4] R. Avery, Theory of coupled reactors, in: proceedings of the 2nd U.N. International conference peaceful uses at. Energy, 12, 1958, pp. 182–191.
[5] M. Boroushaki, M.B. Ghofrani, C. Lucas, M.J. Yazdanpanah, N. Sadati, Axial offset control of PWR nuclear reactor core using intelligent techniques, Nucl. Eng. Des. 227 (2004) 285–300.
[6] R. DeCarlo, S.H. Zak, G.P. Matthews, Variable structure control of nonlinear multivariable systems: a tutorial, IEEE Proc. 76 (1988) 212–232.
[7] Z. Dong, X. Huang, L. Zhang, A nodal dynamic model for control system design and simulation for an MHTGR core, Nucl. Eng. Des. 240 (2010) 1251–1261.
[8] H. Eliasi, M.B. Menhaj, H. Davilu, Robust nonlinear model predictive control for nuclear power plants in load-following operations with bounded xenon oscillations, Nucl. Eng. Des. 241 (2011) 533–543.
[9] David Hetrick, Dynamic of Nuclear Reactor, The University of Chicago press, 1965.
[10] M. Kobayashi, Multi-point Kinetics Equations Using Generalized Perturbation Theory: Physor Seoul, Korea, 2002.
[11] M. Komata, On the derivation of Avery's coupled reactor kinetics equations, Nucl. Scie Eng 38 (1969) 107–118.
[12] C.C. Kuan, C. Lin, C.C. Hsu, Fuzzy logic control of steam generator water level in pressurized water reactors, Nucl. Technol. 100 (1992) 125–134.
[13] P. Ramaswamy, R.M. Edwards, K.Y. Lee, An automatic tuning method of fuzzy logic controller for nuclear reactors, IEEE Transact. Nucl. Sci. 40 (1993) 660–666.
[14] Russia Federal Agency on Nuclear Energy (RFANE), Final Safety Assessment Report (FSAR) for BNPP. Book 1, Moscow, 2005.
[15] Y.B. Shtessel, Sliding mode control of the space nuclear reactor system, IEEE Trans. Aerosp. Electron. Syst. 34 (1998) 579.
[16] P.J. Sipush, R.A. Keer, A.P. Ginsberg, T. Morita, L.R. Scherpereel, Load-follow demonstrations employing constant axial offset power-distribution control procedures, Nucl. Technol. 31 (1976) 12–31.
[17] Jean-Jacques E. Slotine, Weiping Li, Applied Nonlinear Control, Prentice Hall, Upper Saddle River, NJ, 1991.
[18] J.J. Slotine, S.S. Sastry, Tracking control of nonlinear systems using sliding surfaces with application to robot manipulators, Int. J. Control. 38 (1984) 465–492.
[19] V.I. Utkin, Sliding Modes in Control Optimization, Springer, Berlin, 1992.
[20] P. Wang, Z. Chen, R. Zhang, J. Sun, Z. He, F. Zhao, X. Wei, Control simulation and study of load rejection transient for AP1000, Prog. Nucl. Energy 85 (2015) 28–43.
[21] M. Zaidabadi nejad, G.R. Ansarifar, Adaptive robust control for axial offset in the P.W.R nuclear reactors based on the multipoint reactor model during load-following operation, Ann. Nucl. Energy 103 (2017) 251–264.